Surface photovoltage spectroscopy of epitaxial structures for high electron mobility transistors

S. Solodky, A. Khramtsov,[a] T. Baksht, M. Leibovitch,[b] S. Hava,[a] and Yoram Shapira[c]
Department of Physical Electronics, Tel Aviv University, Ramat Aviv 69978, Israel

(Received 18 February 2003; accepted 24 July 2003)

AlGaN/GaN high electron mobility transistor, AlGaAs/InGAs/GaAs pseudomorphic HEMT, and InAlAs/InGaAs metamorphic HEMT (MHEMT) epitaxial structures have been characterized using surface photovoltage spectroscopy. The effects of the transistor top and bottom delta-doping levels δ_{top}, δ_{bot}, and surface charge Q_{sur} on the spectrum features have been studied using numerical simulations. Based on the latter, an empirical model has been developed, which allows extraction and comparison of δ_{top}, δ_{bot}, and Q_{sur} and is applicable for both double-sided and single-sided delta-doped structures. Prediction of the final device performance by the model is shown for two MHEMT structures. Devices produced on these structures show maximum drain currents, which correlate well with δ_{top} values calculated using the model. © *2003 American Institute of Physics.* [DOI: 10.1063/1.1613794]

GaN/AlGaN high electron mobility transistors (HEMTs) have been very promising for high power high-speed applications[1] due to their high electron mobility of two-dimensional electron gas (2DEG), good thermal isolation, and high breakdown voltage. High cutoff and maximum oscillation frequencies[2,3] together with low-cost GaAs substrates make metamorphic HEMTs (MHEMTs) attractive for low-noise applications. InGaAs/GaAs pseudomorphic HEMTs (PHEMTs) are the current ''work horses,'' widely used for microwave, high speed and power applications.[4]

The interplay of epitaxial structure parameters and lateral geometry parameters of a transistor defines the distribution of electric fields within the device and thus its electrical performance. The top and bottom delta-doping levels, δ_{top} and δ_{bot}, together with the surface and interface charge densities Q_{sur} and Q_{int} and layer thickness define the distribution of the vertical electric fields within the device and the electron sheet density in the channel. They affect the final dc and rf device parameters. Thus, it is crucially important to develop a methodology capable of predicting eventual device performance based on monitoring epistructure parameters. Such a methodology should be contactless, nondestructive, wafer-scalable, and usable for structures with different material compositions. Indeed, photoluminescence[5,6] electroreflectance, photoreflectance,[7] and x-ray microscopy[8] have been used for the characterization of HEMT structures.

Surface photovoltage spectroscopy (SPS) is a method, which fulfills most of the demands for comprehensive transistor structure characterization and for incoming wafer inspection.[9] SPS monitors changes in the semiconductor surface work function induced by absorption of monochromatic light, giving rise to surface photovoltage (SPV). A detailed description of this method and its applications may be found in Ref. 10. This technique has been successfully applied for characterization of structures and devices.[11–15] Recently, Cheng *et al.* reported on SPS characterization of PHEMT structures.[16] Signals have been observed from every region of the sample. From a line shape fit of the SPV signal with respect to the photon energy, the authors obtain the 2DEG density. The Al composition of the GaAs/AlGaAs superlattice buffer as well as the intersubband transition energies of the buffer and channel layer have been deduced from the experiment. However, the authors do not refer to electrical field and charge distributions in the epistructures with different material composition and different band lineups and their correlation with the final device performance.

In this letter, we present a methodology of contactless characterization of various HEMT structures. This approach is based on deep analysis of HEMT SPV spectra together with numerical simulations of spectral features and empirical modeling. The empirical model is applied to characterization of differences in doping level between various GaN/AlGaN HEMT, MHEMT, and PHEMT structures. dc characterization of final devices has been performed.

HEMT structures have been fabricated by metalorganic chemical vapor deposition (MOCVD) and molecular beam epitaxy (MBE) growth techniques. Table I summarizes the material composition and range of doping levels of the struc-

TABLE I. Materials properties of studied HEMT structures.

	PHEMT	MHEMT	AlGaN/GaN HEMT
Growth technique	MBE	MBE	MOCVD
Substrate	GaAs	GaAs	SiC
Channel	$In_{0.2}Ga_{0.8}As$	$In_{0.5}Ga_{0.5}As$	GaN
Buffer	GaAs-AlGaAs	InAlAs	GaN
Schottky layer	AlGaAs	InAlAs	AlGaN
Top delta-doping	$3-6\times10^{12}$ cm^{-2}	$3-6\times10^{12}$ cm^{-2}	1×10^{13} cm^{-2}
Bottom delta-doping	$0.4-1.5\times10^{12}$ cm^{-2}	$0.4-1.5\times10^{12}$ cm^{-2}	⋯

[a]Also at: Department of Electrical and Computer Engineering, Ben-Gurion University, Beer-Sheva 84105, Israel.
[b]Also at: Gal-El (MMIC), P.O. Box 330, Ashdod 77102, Israel.
[c]Electronic mail: shapira@eng.tau.ac.il

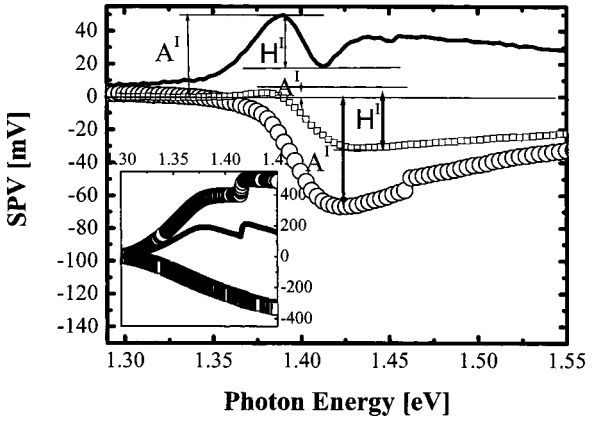

FIG. 1. Typical surface photovoltage spectra of a PHEMT (solid curve) and two MHEMT structures: $M1$ (circles) and $M2$ (squares). Labels correspond to the spectrum parameterization scheme: A^I—first peak amplitude, H^I—first peak height. Inset: Simulated SPV signal from a double-sided delta-doped PHEMT structure (solid curve) together with simulated signals from buffer (circles) and Schottky layer (squares).

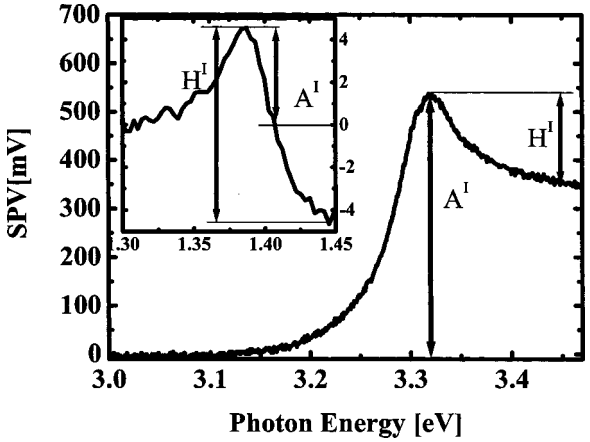

FIG. 2. Surface photovoltage spectra of two single-sided doped structures GaN HEMT and MHEMT (inset).

tures as given by the manufacturer. SPS experiments have been performed in air using a commercial Kelvin probe unit with a sensitivity of ~ 1 mV.

The SPV spectra analysis is based on quantitative simulations, numerically solving the Poisson equation, the Schrödinger equation, the continuity equations for electrons and holes and the current equations.[17] Typical HEMT structures are designed in such a way that there are two oppositely directed electric fields in the buffer, a wide layer grown on the substrate that is introduced to prevent substrate defects from reaching the active region of the device, and in the Schottky layer, an undoped layer that separates between the gate and the channel.[18] Thus, the SPV signals from these layers are of opposite signs. The total SPV signal is a combination of the signals from all structure layers. The signal magnitude is a complicated function of light absorption and the electric fields in any absorption region. Absorption of light in the quantum well (QW) creates electron-hole pairs. While electrons are confined within the QW by fields in buffer and Schottky layer, holes are likely to overcome the QW–Schottky layer interface or the QW-buffer interface potential barrier. The holes are swept by the electric field in the buffer or in the Schottky layer direction, contributing to signals with opposite signs. The inset in Fig. 1 shows the simulated SPV signal from the buffer (circles), the Schottky layer (squares) as well as the total signal (solid curve) for a double-sided delta-doped PHEMT structure. In the simulated case, at photon energies below 1.37 eV the signal from the buffer is dominant, which results in a positive total SPV. When the signal from the buffer is saturated, the total SPV changes sign because of the dominating signal from the Schottky layer. The absorption in the buffer is the reason for the second peak formation. In a GaN/AlGaN HEMT structure, a triangular QW is formed at the interface with Schottky layer. Thus, the potential barrier for holes is much smaller in the Schottky layer direction and holes generated by QW absorption are swept toward the Schottky layer, contributing to a dominant positive signal in the QW region of absorption.

Figure 1 shows parts of SPV spectra of a double-sided delta-doped PHEMT structure (solid curve) and two MHEMT structures, $M1$ (circles) and $M2$ (squares), which differ in their top delta-doping δ_{top} levels. Differences in δ_{top} between the structures lead to changes in electric fields distributions and potential profiles, which, in turn, lead to variations of spectral shapes between the structures. At the low energy region, absorption takes place in the QW. At this portion of the spectrum, increasing signals (for PHEMT and $M2$ spectra) as well as decreasing signals (for $M1$) are observed. At energies above 1.4 eV, a second peak in the PHEMT spectrum is observed. This feature may be attributed to GaAs absorption. At low photon energies, Fermi filling, due to high electron concentration in the channel, dominates the InGaAs absorption coefficient.[19] This effect significantly changes the absorption coefficient of the QW by blueshifting its edge and reducing its magnitude at higher energies.

Figure 2 shows SPV spectra of a single-sided delta-doped GaN HEMT and a MHEMT (see inset of Fig. 2). The total signal in the QW absorption region is positive. Therefore, SPV spectra of double-sided and single-sided delta-doped structures with different material composition may be fully understood.

The spectra of HEMT structures were parameterized (see Figs. 1 and 2). The spectral parameters are the amplitude of the first peak (or minimum) A^I and the peak height H^I. The signal amplitude is defined by the overall electric fields distribution in the structure, which is dictated by δ_{top}, δ_{bot}, and Q_{sur}. Thus, A^I depends on all charges densities in the structure. H^I is a result of the strong interplay between the PV from the Schottky and buffer layers. This interplay depends on the electric field distribution in the buffer and Schottky layers, which is defined by δ_{top} and δ_{bot}.

The empirical model, which correlates between the spectral features A^I, H^I and the structural parameters δ_{top}, δ_{bot}, and Q_{sur} has been developed using numerical simulations. This model has been applied to several PHEMT structures and the efficiency of the model for PHEMT characterization is shown in Ref. 15. δ_{top}, δ_{bot}, and Q_{sur} are changed in the simulated structures and their effects on A^I and H^I from simulated spectra have been analyzed. A two-level factorial design[15,20,21] has been used to define the device structure with different combinations of structural parameters. Detailed description of the modeling procedure and the model

coefficients are given in Ref. 15. The model shows that the differences in a spectral parameter A^J (relative to a reference structure) is given by

$$\Delta A^J(\delta_{\text{top}},\delta_{\text{bot}},Q_{\text{sur}}) = C_{\delta\text{top}}\Delta\delta_{\text{top}} + C_{\delta\text{bot}}\Delta\delta_{\text{bot}} + C_{Q\text{sur}}\Delta Q_{\text{sur}}, \quad (1)$$

where $C_{\delta\text{top}}$, $C_{\delta\text{bot}}$, $C_{Q\text{sur}}$ are coefficients, which weight the influence of each of the electrical parameters on the spectral parameter A^J. Here we present the capability of the model to characterize HEMT structures with different material composition and to predict final device performance.

Spectra of double-sided delta-doped HEMT (represented by the solid curve in Fig. 1) and MHEMT (dotted curve) were compared. The δ_{top} in the PHEMT structure is 5×10^{12} cm^{-2}. The structures have the same δ_{bot} level and the difference in δ_{top} specified by the supplier is 1×10^{12} cm^{-2}. Variations in δ_{top} change the electric field distribution in the Schottky layer region and thus the spectral shapes of the QW absorption region significantly differ. The difference in δ_{top} has been calculated using the model. Q_{sur} is assumed to be the same, which reduces Eq. (1) to $\Delta A^I = 130\Delta\delta_{\text{top}}$. The calculated $\Delta\delta_{\text{top}}$ is 0.9×10^{12} cm^{-2}, which is in good agreement with the grower specifications. Two single-sided top-delta-doping structures of GaN/AlGaN HEMT and MHEMT have been compared using the empirical model. In these HEMTs, $\delta_{\text{top}}=1.0\times10^{13}$ cm^{-2} and 0.6×10^{13} cm^{-2}, respectively. The value of $\Delta\delta_{\text{top}}$ calculated from the model is 4.4×10^{12} cm^{-2}, which is in good agreement with the supplier specifications.

Therefore, the model developed for double-sided delta-doped PHEMT structures accounts well for differences in δ_{top} of GaN HEMT and MHEMT structures. This model is applicable for double-sided delta-doped as well as for single-sided delta-doped structures. It shows that this is a universal empirical model, sensitive to differences in doping levels for a wide variety of HEMT structures.

Demonstrating the capability of this methodology to predict the final device performance, two MHEMT structures have been characterized by SPS and consequently complete devices have been fabricated on the substrates. The differences in delta-doping levels indicate variations in the channel sheet density n_s, where n_s defines a maximum current I_{max} for a given device.[22] Therefore, by monitoring differences in the delta-doping levels, difference in the final device performance may be predicted.

The model has been applied to the two double-sided delta-doped MHEMT structures, $M1$ and $M2$, whose spectra are shown by the circles and squares, respectively in Fig. 1. The δ_{bot} is the same for both structures while $\Delta\delta_{\text{top}}$, as given by the grower is 0.5×10^{12} cm^{-2}. The value calculated from the model is $\Delta\delta_{\text{top}}=0.3\times10^{12}$ cm^{-2}, which corresponds to a relative change of 7.5%. Devices produced on $M1$ and $M2$ structures have been characterized. A relative difference of 8.2% in I_{max} was measured correlating with the difference in δ_{top} extracted from the model. This demonstrates the sensitivity of our methodology to even slight differences in the delta-doping level, allows prediction of the device dc and power performance.

In conclusion, GaN/AlGaN HEMT, MHEMT, and PHEMT epitaxial structures have been characterized by SPS. Effects of δ_{top}, δ_{bot}, and Q_{sur} on SPV spectra were found, using numerical simulations. A complete empirical model providing doping levels has been developed. The universality of the model for characterization of HEMT structures of various material compositions is shown. The capability of characterization using SPS to predict the final device performance has been demonstrated for MHEMT structures.

Y.S. is indebted to the Krongold family for their generous support in establishing the Krongold Chair of Microelectronics.

[1] J. Bernat, A. Fox, P. Javorka, P. Kordos, M. Marso, M. Wolter, Proc. GaAs Manufacturing Technology (MANTECH) Conference, San Diego, CA, 8–11 April 2002, p. 243.
[2] Y. Yamashita, A. Endoh, K. Shinohara, M. Higashiwaki, K. Hikosaka, T. Mimura, S. Hiyamizu, and T. Matsui, IEEE Electron Device Lett. **22**, 367 (2001).
[3] S. Bollaert, Y. Cordier, M. Zaknoune, T. Parenty, H. Happy, S. Lepilliet, and A. Cappy, Electron. Lett. **38**, 389 (2002).
[4] S. A. Brown and J. M. Carroll, Proc. GaAS IC Manufacturing Technology (MANTECH) Conference, Seattle, WA, 5–8 Nov. 2000, p. 223.
[5] K. Radhakrisnan, T. H. K. Patrick, H. Q. Zheng, P. H. Zhang, and S. F. Ynon, Microelectron. Eng. **51–52**, 441 (2000).
[6] C. Y. Fang, C. F. Lin, E. Y. Chang, and M. S. Feng, Appl. Phys. Lett. **80**, 4558 (2002).
[7] F. H. Pollak, Mater. Sci. Eng., B **80**, 178 (2001).
[8] A. Torabi, P. Ericson, E. J. Yarranton, and W. E. Hoke, J. Vac. Sci. Technol. B **20**, 1234 (2002).
[9] Y. T. Cheng, Y. Huang, D. Y. Lin, F. H. Pollak, and K. R. Evans, Physica E (Amsterdam) **14**, 313 (2002).
[10] L. Kronik and Y. Shapira, Surf. Interface Anal. **31**, 954 (2001).
[11] B. Mishori, M. Leibovitch, Y. Shapira, F. H. Pollak, D. C. Streit, and M. Wojtowicz, Appl. Phys. Lett. **73**, 650 (1998).
[12] N. Bachrach-Ashkenasy, L. Kronik, Y. Shapira, Y. Rosenwaks, M. C. Hanna, M. Leibovitch, and P. Ram, Appl. Phys. Lett. **68**, 879 (1996).
[13] N. Ashkenasy, M. Leibovitch, Y. Shapira, F. H. Pollak, T. Burnham, and X. Wang, J. Appl. Phys. **83**, 1146 (1998).
[14] N. Ashkenasy, M. Leibovitch, Y. Rosenwaks, Y. Shapira, K. W. J. Barnham, J. Nelson, and J. Barnes, J. Appl. Phys. **86**, 6902 (1999).
[15] S. Solodky, N. Ashkenasy, M. Leibovitch, I. Hallakoun, Y. Rosenwaks, and Y. Shapira, J. Appl. Phys. **88**, 6775 (2000).
[16] Y. T. Cheng, Y. S. Huang, D. Y. Lin, K. K. Tiong, F. H. Pollak, and K. R. Evans, Appl. Phys. Lett. **79**, 949 (2001).
[17] G. A. Ashkinazi, M. G. Leibovitch, and M. Nathan, IEEE Trans. Electron Devices **40**, 285 (1993).
[18] W. E. Quinn, B. Lauterwasser, J. Kronwasser, T. Mizandi and D. Carlson, Proc. Gats Manufacturing Technology (MANTECH) Conference, San Franscisco, CA, 2–5 June 1997, p. 166.
[19] Y. H. Zhang and K. Ploog, Phys. Rev. B **45**, 14069 (1992).
[20] H. G. Henry and K. M. Renaldo, Proc. Gats Manufacturing Technology (MANTECH) Conference, Seattle, WA, 27–30 April 1998, p. 195.
[21] G. E. P. Box, W. J. Hunter, and J. S. Hunter, *Statistics for Experiments* (Wiley, New York, 1978).
[22] C. Weisbuch and B. Vinter, *Quantum Semiconductor Structures* (Academic, New York, 1991).